VNU Journal of Science: Mathematics – Physics, Vol. 35, No. 4 (2019) 1-21

VNU Journal of Science: Mathematics - Physics

Journal homepage: https://js.vnu.edu.vn/MaP

Original Article

Nonlinear Vibration of Porous Funcationally Graded Cylindrical Panel Using Reddy's High Order Shear Deformation

Vu Minh Anh[1], Nguyen Dinh Duc[1,2,*]

[1]*Department of Construction and Transportation Engineering, VNU University of Engineering and Technology, 144 Xuan Thuy, Cau Giay, Hanoi, Vietnam*

[2]*Infrastructure Engineering Program, VNU Vietnam-Japan University (VJU), My Dinh 1, Tu Liem, Hanoi, Vietnam*

Received 02 December 2019
Accepted 06 December 2019

Abstract: The nonlinear dynamic response and vibration of porous functionally graded cylindrical panel (PFGCP) subjected to the thermal load, mechanical load and resting on elastic foundations are determined by an analytical approach as the Reddy's third order shear deformation theory, Ahry's function… The study results for dynamic response of PFGCP present the effect of geometrical ratio, elastic foundations: Winkler foundation and Paskternak foundation; loads: mechanical load and thermal load; and the material properties and distribution type of porosity. The results are shown numerically and are determined by using Galerkin methods and Fourth-order Runge-Kutta method.

Keywords: Nonlinear dynamic response, porous functionally graded cylindrical panel, the high order shear deformation theory, mechanical load, thermal load, nonlinear vibration.

1. Introduction

With the requirements of working ability such as bearing, high temperature in the harsh environment of some key industries such as defense industries, aircraft, space vehicles, reactor vessels and other engineering structures, in the world, many advanced materials have appeared, including Functionally Graded Materials (FGMs). FGMs is a composites material and is made by a combination of two main materials: metal and ceramic. Therefore, the material properties of FGMs will have all the

*Corresponding author.
Email address: ducnd@vnu.edu.vn

https//doi.org/ 10.25073/2588-1124/vnumap.4444

outstanding properties of the two-component materials and vary with the thickness of the structure. With these outstanding properties, FGMs have attracted the attention of scientists in the world. In recent years, a lot of research carried out on FGMs, dynamic FGMs.

Contact mechanics of two elastic spheres reinforced by functionally graded materials

(FGM) thin coatings are studied by Chen and Yue [1] . Li et al. [2] determined nonlinear structural stability performance of pressurized thin-walled FGM arches under temperature variation field. Dastjerdi and Akgöz [3] presented new static and dynamic analyses of macro and nano FGM plates using exact three-dimensional elasticity in thermal environment. Wang and Zu [4] researched about nonlinear dynamic thermoelastic response of rectangular FGM plates with longitudinal velocity. Dynamic response of an FGM cylindrical shell under moving loads is investigated by Sofiyev [5]. Wang and Shen [6] published nonlinear dynamic response of sandwich plates with FGM face sheets resting on elastic foundations in thermal environments. Shariyat [7] gave vibration and dynamic buckling control of imperfect hybrid FGM plates with temperature-dependent material properties subjected to thermo-electro-mechanical loading conditions. Nonlinear dynamic analysis of sandwich S- FGM plate resting on pasternak foundation under thermal environment are reseached by Singh and Harsha [8]. Nonlinear dynamic buckling of the imperfect orthotropic E- FGM circular cylindrical shells subjected to the longitudinal constant velocity are studied by Gao [9]. Reddy and Chin [10] studied thermo-mechanical analysis of functionally graded cylinders and plates. Babaei et al. [11] investigated thermal buckling and post-buckling analysis of geometrically imperfect FGM clamped tubes on nonlinear elastic foundation. 3D graphical dynamic responses of FGM plates on Pasternak elastic foundation based on quasi-3D shear and normal deformation theory is presented by Han et al [12]. Ghiasian et al. [13] researched about dynamic buckling of suddenly heated or compressed FGM beams resting on nonlinear elastic foundation. Geometrically nonlinear rapid surface heating of temperature-dependent FGM arches are gave by Javani et al. [14]. Shariyat [15] presented dynamic thermal buckling of suddenly heated temperature-dependent FGM cylindrical shells, under combined axial compression and external pressure. Babaei et al. [16] published large amplitude free vibration analysis of shear deformable FGM shallow arches on nonlinear elastic foundation.

In fact, porous materials appear around us and play in many areas of life such as fluid filtration, insulation, vibration dampening, and sound absorption. In addition, porous materials have high rigidity leading to the ability to work well in harsh environments. In recent years, porous materials have been researched and applied along with other materials to create new materials with the preeminent properties of component materials. Porous functionally graded (PFG) is one of the outstanding materials among them and has research works such as: Gao et al. [17] researched about dynamic characteristics of functionally graded porous beams with interval material properties. Dual-functional porous copper films modulated via dynamic hydrogen bubble template for in situ SERS monitoring electrocatalytic reaction are proposed by Yang et al. [18]. Foroutan et al. [19] investigated nonlinear static and dynamic hygrothermal buckling analysis of imperfect functionally graded porous cylindrical shells. Li [20] presented nonlinear vibration and dynamic buckling analyses of sandwich functionally graded porous plate with graphene platelet reinforcement resting on Winkler–Pasternak elastic foundation. Li [21] carried out experimental research on dynamic mechanical properties of metal tailings porous concrete. Transient [22] published response of porous FG nanoplates subjected to various pulse loads based on nonlocal stress-strain gradient theory. Esmaeilzadeh and Kadkhodayan [23] researched about dynamic analysis of stiffened bi-directional functionally graded plates with porosities under a moving load by dynamic relaxation method with kinetic damping. Vibration analysis of magneto-electro-elastic heterogeneous porous material plates resting on elastic foundations are studied by Ebrahimi et al [24]. Arshid and Khorshidvand [25] presented free vibration analysis of saturated porous FG circular plates integrated with piezoelectric actuators via differential quadrature

method. Micro temperature-dependent FG porous plate: Free vibration and thermal buckling analysis using modified couple stress theory with CPT and FSDT are researched by Shojaeefard [26]. Demirhan and Taskin [27] investigated bending and free vibration analysis of Levy-type porous functionally graded plate using state space approach.

The proposed method used in this study is the third-order shear deformation theory and the effect of the thermal load has been applied in a number of case studies such as Zhang [28] published nonlinear bending analysis of FGM beams based on physical neutral surface and high order shear deformation theory. Reddy and Chin [29] investigated thermo-mechanical analysis of functionally graded cylinders and plates. Modeling and analysis of FGM rectangular plates based on physical neutral surface and high order shear deformation theory is presented by Zang [30]. In [31], Thon and Bélanger presented EMAT design for minimum remnant thickness gauging using high order shear horizontal modes. Dynamic analysis of composite sandwich plates with damping modelled using high order shear deformation theory are carried out by Meunier and Shenoi [32]. Cong et al.[33] investigated nonlinear dynamic response of eccentrically stiffened FGM plate using Reddy's TSDT in thermal environment. Stability of variable thickness shear deformable plates—first order and high order analyses are gave by Shufrin and M. Eisenberger [34]. In [35], Stojanović et al showed exact closed-form solutions for the natural frequencies and stability of elastically connected multiple beam system using Timoshenko and high order shear deformation theory. A high order shear element for nonlinear vibration analysis of composite layered plates and shells are proposal by Attia and El-Zafrany [36]. Khoa et al [37] observed nonlinear dynamic response and vibration of functionally graded nanocomposite cylindrical panel reinforced by carbon nanotubes in thermal environment. In [38], Allahyari and Asgari found that thermo-mechanical vibration of double-layer graphene nanosheets in elastic medium considering surface effects; developing a nonlocal third order shear deformation theory. Wang and Shi [39] presented a refined laminated plate theory accounting for the third order shear deformation and interlaminar transverse stress continuity.

From the literature review, the authors often used the high order shear deformation theory to investigate the nonlinear static, nonlinear dynamic or nonlinear vibration of FGM or plate porous funcationally graded (PFG). For the nonlinear dynamic and vibration of PFGCP has not carried out. Therefore, in order to observe the nonlinear dynamic and vibration of PFGCP under mechanical load and thermal load, using the Reddy's high order shear deformation theory and Ahry' function are proposaled in this paper. The natural frequency of PFGCP is obtained by using cylindrical panel fourth-order Runge-Kutta method. Besides, the effect of geometrical ratio, elastic foundations: Winkler foundation and Paskternak foundation, the material properties and distribution type of porous on the modeling will be shown.

2. Theoretical formulation

Fig.1 show a PFGCP resting on elastic foundations included Winkler foundation and Pasternak foundation in a Cartesian coordinate system x, y, z , with

xy - the midplane of the panel

z - the thickness coordinator, $-h/2 \le z \le h/2$.

a - the length

b - the width

h - the thickness of the panel.

R - the radius of the cylinderical panel.

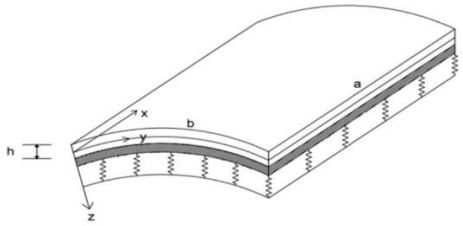

Fig. 1. Geometry of the PFGCP on elastic foundation.

The volume fractions of metal and ceramic, V_m and V_c, are assumed as [25] with using a simple power-law distribution:

$$V_c(z)=\left(\frac{2z+h}{2h}\right)^N;V_m(z)=1-V_c(z), \tag{1}$$

in which the volume fraction index N, subscripts m and c stand for the metal and ceramic constituents, respectively.

The material properties of PFGCP with prosity distribution are given as

Porosity – I:

$$\begin{aligned}&\left[E(z),\alpha(z),\rho(z)\right]=\left[E_m,\alpha_m,\rho_m\right]\\&+\left[E_{cm},\alpha_{cm},\rho_{cm}\right]\left(\frac{2z+h}{2h}\right)^N-\frac{\alpha}{2}\left[E_m+E_c,\alpha_m+\alpha_c,\rho_m+\rho_c\right],\end{aligned} \tag{2}$$

Porosity – II:

$$\begin{aligned}&\left[E(z),\alpha(z),\rho(z)\right]=\left[E_m,\alpha_m,\rho_m\right]\\&+\left[E_{cm},\alpha_{cm},\rho_{cm}\right]\left(\frac{2z+h}{2h}\right)^N-\frac{\alpha}{2}\left(1-2\frac{|z|}{h}\right)\left[E_m+E_c,\alpha_m+\alpha_c,\rho_m+\rho_c\right],\end{aligned} \tag{3}$$

with

$$E_{cm}=E_c-E_m,\ \alpha_{cm}=\alpha_c-\alpha_m,\ \rho_{cm}=\rho_c-\rho_m,K_{cm}=K_c-K_m, \tag{4}$$

and in this paper, the Poisson ratio $\nu(z)$ can be considered constant $\nu(z)=\nu$.

a. Porosity - I b. Porosity - II

Fig. 2. The porosity distribution type.

2.1. Governing equations

By using the Reddy's high order shear deformation theory (HSDT), the governing equations and the dynamic analysis of PFGCP are determined.

The train-displacement relations taking into account the Von Karman nonlinear terms as [10,29,33]:

$$\begin{pmatrix}\varepsilon_x\\ \varepsilon_y\\ \gamma_{xy}\end{pmatrix}=\begin{pmatrix}\varepsilon_x^0\\ \varepsilon_y^0\\ \gamma_{xy}^0\end{pmatrix}+z\begin{pmatrix}k_x^1\\ k_y^1\\ k_{xy}^1\end{pmatrix}+z^3\begin{pmatrix}k_x^3\\ k_y^3\\ k_{xy}^3\end{pmatrix};\begin{pmatrix}\gamma_{xz}\\ \gamma_{yz}\end{pmatrix}=\begin{pmatrix}\gamma_{xz}^0\\ \gamma_{yz}^0\end{pmatrix}+z^2\begin{pmatrix}k_{xz}^2\\ k_{yz}^2\end{pmatrix}, \tag{5}$$

With

$$\begin{pmatrix}\varepsilon_x^0\\ \varepsilon_y^0\\ \gamma_{xy}^0\end{pmatrix}=\begin{pmatrix}\dfrac{\partial u}{\partial x}+\dfrac{w}{R}+\dfrac{1}{2}\left(\dfrac{\partial w}{\partial x}\right)^2\\ \dfrac{\partial v}{\partial y}+\dfrac{1}{2}\left(\dfrac{\partial w}{\partial y}\right)^2\\ \dfrac{\partial u}{\partial y}+\dfrac{\partial v}{\partial x}+\dfrac{\partial w}{\partial x}\dfrac{\partial w}{\partial y}\end{pmatrix};\begin{pmatrix}k_x^1\\ k_y^1\\ k_{xy}^1\end{pmatrix}=\begin{pmatrix}\dfrac{\partial \phi_x}{\partial x}\\ \dfrac{\partial \phi_y}{\partial y}\\ \dfrac{\partial \phi_x}{\partial y}+\dfrac{\partial \phi_y}{\partial x}\end{pmatrix};$$

$$\begin{pmatrix}k_x^3\\ k_y^3\\ k_{xy}^3\end{pmatrix}=-c_1\begin{pmatrix}\dfrac{\partial \phi_x}{\partial x}+\dfrac{\partial^2 w}{\partial x^2}\\ \dfrac{\partial \phi_y}{\partial y}+\dfrac{\partial^2 \mathrm{w}}{\partial y^2}\\ \dfrac{\partial \phi_x}{\partial y}+\dfrac{\partial \phi_y}{\partial x}+2\dfrac{\partial^2 \mathrm{w}}{\partial x\partial y}\end{pmatrix}, \tag{6}$$

$$\begin{pmatrix}\gamma_{xz}^0\\ \gamma_{yz}^0\end{pmatrix}=\begin{pmatrix}\phi_x+\dfrac{\partial \mathrm{w}}{\partial x}\\ \phi_y+\dfrac{\partial \mathrm{w}}{\partial y}\end{pmatrix};\begin{pmatrix}k_{xz}^2\\ k_{yz}^2\end{pmatrix}=-3c_1\begin{pmatrix}\phi_x+\dfrac{\partial \mathrm{w}}{\partial x}\\ \phi_y+\dfrac{\partial \mathrm{w}}{\partial y}\end{pmatrix},$$

in which

$c_1=4/3h^2, \varepsilon_x, \varepsilon_y$

$\varepsilon_x, \varepsilon_y$ - normal strains,

γ_{xy} - the in-plane shear strain,

γ_{xz}, γ_{yz} - the transverse shear deformations

u, v, w - the displacement components along the x, y, z directions, respectively

ϕ_x, ϕ_y - the slope rotations in the (x,z) and (y,z) planes, respectively.

The strains are related in the compatibility equation [27, 28]:

$$\frac{\partial^2 \varepsilon_x^0}{\partial y^2}+\frac{\partial^2 \varepsilon_y^0}{\partial x^2}-\frac{\partial^2 \gamma_{xy}^0}{\partial x \partial y}=\left(\frac{\partial^2 \mathrm{w}}{\partial x \partial y}\right)^2-\frac{\partial^2 \mathrm{w}}{\partial x^2}\frac{\partial^2 \mathrm{w}}{\partial y^2}-\frac{1}{R}\frac{\partial^2 \mathrm{w}}{\partial x^2}. \tag{7}$$

The effect of temperature will be descirbed in Hooke's law for a PFGCP as:

$$\begin{aligned}&\left(\sigma_x,\sigma_y\right)=\frac{E}{1-\nu^2}[(\varepsilon_x,\varepsilon_y)+\nu\left(\varepsilon_y,\varepsilon_x\right)-(1+\nu)\alpha\Delta T(1,1)],\\&\left(\sigma_{xy},\sigma_{xz},\sigma_{yz}\right)=\frac{E}{2(1+\nu)}\left(\gamma_{xy},\gamma_{xz},\gamma_{yz}\right),\end{aligned} \tag{8}$$

in which ΔT is temperature rise.

The force and moment resultants of the PFGCP can be obtained with equations of stress components along with thickness of PFGCP as:

$$\begin{aligned}&\left(N_i,M_i,P_i\right)=\int_{-h/2}^{h/2}\sigma_i\left(1,z,z^3\right)dz;i=x,y,xy,\\&\left(Q_i,R_i\right)=\int_{-h/2}^{h/2}\sigma_j(1,z^2)dz;i=x,y;\ j=xz,yz.\end{aligned} \tag{9}$$

Replacing Eqs. (3), (5) and (8) into Eq. (9) gives:

$$\begin{aligned}&\left(N_x,M_x,P_x\right)=\frac{1}{1-\nu^2}\left[\begin{matrix}\left(E_1,E_2,E_4\right)\left(\varepsilon_x^0+\nu\varepsilon_y^0\right)+\left(E_2,E_3,E_5\right)\left(k_x^1+\nu k_y^1\right)\\+\left(E_4,E_5,E_7\right)\left(k_x^3+\nu k_y^3\right)-(1+\nu)\left(\Phi_a,\Phi_b,\Phi_c\right)\end{matrix}\right],\\&\left(N_y,M_y,P_y\right)=\frac{1}{1-\nu^2}\left[\begin{matrix}\left(E_1,E_2,E_4\right)\left(\varepsilon_y^0+\nu\varepsilon_x^0\right)+\left(E_2,E_3,E_5\right)\left(k_y^1+\nu k_x^1\right)\\+\left(E_4,E_5,E_7\right)\left(k_y^3+\nu k_x^3\right)-(1+\nu)\left(\Phi_a,\Phi_b,\Phi_c\right)\end{matrix}\right],\\&\left(N_{xy},M_{xy},P_{xy}\right)=\frac{1}{2(1+\nu)}\left[\left(E_1,E_2,E_4\right)\gamma_{xy}^0+\left(E_2,E_3,E_5\right)k_{xy}^1+\left(E_4,E_5,E_7\right)k_{xy}^3\right],\\&\left(Q_x,R_x\right)=\frac{1}{2(1+\nu)}\left[\left(E_1,E_3\right)\gamma_{xz}^0+\left(E_3,E_5\right)k_{xz}^2\right],\\&\left(Q_y,R_y\right)=\frac{1}{2(1+\nu)}\left[\left(E_1,E_3\right)\gamma_{yz}^0+\left(E_3,E_5\right)k_{yz}^2\right],\end{aligned} \tag{10}$$

with

$$\begin{aligned}&\left(E_1,E_2,E_3,E_4,E_5,E_7\right)=\int_{-h/2}^{h/2}\left(1,z,z^2,z^3,z^4,z^6\right)E(z)dz,\\&(\Phi_a,\Phi_b,\Phi_c)=\int_{-h/2}^{h/2}(1,z,z^3)E(z)\alpha(z)\Delta T(z)dz,\end{aligned} \tag{11}$$

and the coefficients $E_i(i=1\div 5,7)$ are give in Appendix.

From Eq. (10), The inverse expression are obtained:

$$\varepsilon_x^0 = \frac{1}{E_1}\left[N_x - \nu N_y - E_2 k_x^1 - E_4 k_x^3 + \Phi_a \right]; \varepsilon_y^0 = \frac{1}{E_1}\left[N_y - \nu N_x - E_2 k_y^1 - E_4 k_y^3 + \Phi_a \right],$$
$$\gamma_{xy}^0 = \frac{1}{E_1}\left[2(1+\nu) N_{xy} - E_2 k_{xy}^1 - E_4 k_{xy}^3 \right]. \quad (12)$$

The equations of motion are [26] based on HSDT:

$$\frac{\partial N_x}{\partial x} + \frac{\partial N_{xy}}{\partial y} = I_0 \frac{\partial^2 u}{\partial t^2} + J_1 \frac{\partial^2 \phi_x}{\partial t^2} - c_1 I_3 \frac{\partial^3 \mathrm{w}}{\partial x \partial t^2},$$
$$\frac{\partial N_{xy}}{\partial x} + \frac{\partial N_y}{\partial y} = I_0 \frac{\partial^2 v}{\partial t^2} + J_1 \frac{\partial^2 \phi_y}{\partial t^2} - c_1 I_3 \frac{\partial^3 \mathrm{w}}{\partial y \partial t^2},$$
$$\frac{\partial Q_x}{\partial x} + \frac{\partial Q_y}{\partial y} - c_2 \left(\frac{\partial R_x}{\partial x} + \frac{\partial R_y}{\partial y} \right) + N_x \frac{\partial^2 \mathrm{w}}{\partial x^2} + 2N_{xy} \frac{\partial^2 \mathrm{w}}{\partial x \partial y} + N_y \frac{\partial^2 \mathrm{w}}{\partial y^2}$$
$$+ c_1 \left(\frac{\partial^2 P_x}{\partial x^2} + 2\frac{\partial^2 P_{xy}}{\partial x \partial y} + \frac{\partial^2 P_y}{\partial y^2} \right) - k_1 \mathrm{w} + k_2 \left(\frac{\partial^2 \mathrm{w}}{\partial x^2} + \frac{\partial^2 \mathrm{w}}{\partial y^2} \right) + \frac{N_y}{R} + q$$
$$= I_0 \frac{\partial^2 \mathrm{w}}{\partial t^2} + 2\varepsilon I_0 \frac{\partial \mathrm{w}}{\partial t} - c_1^2 I_6 \left(\frac{\partial^4 \mathrm{w}}{\partial x^2 \partial t^2} + \frac{\partial^4 \mathrm{w}}{\partial y^2 \partial t^2} \right)$$
$$+ c_1 \left[I_3 \left(\frac{\partial^3 u}{\partial x \partial t^2} + \frac{\partial^3 v}{\partial y \partial t^2} \right) + J_4 \left(\frac{\partial^3 \phi_x}{\partial x \partial t^2} + \frac{\partial^3 \phi_y}{\partial y \partial t^2} \right) \right], \quad (13)$$
$$\frac{\partial M_x}{\partial x} + \frac{\partial M_{xy}}{\partial y} - c_1 \left(\frac{\partial P_x}{\partial x} + \frac{\partial P_{xy}}{\partial y} \right) - Q_x - c_2 R_x = J_1 \frac{\partial^2 u}{\partial t^2} + K_2 \frac{\partial^2 \phi_x}{\partial t^2} - c_1 J_4 \frac{\partial^3 \mathrm{w}}{\partial x \partial t^2},$$
$$\frac{\partial M_{xy}}{\partial x} + \frac{\partial M_y}{\partial y} - c_1 \left(\frac{\partial P_{xy}}{\partial x} + \frac{\partial P_y}{\partial y} \right) - Q_y - c_2 R_y = J_1 \frac{\partial^2 v}{\partial t^2} + K_2 \frac{\partial^2 \phi_y}{\partial t^2} - c_1 J_4 \frac{\partial^3 \mathrm{w}}{\partial y \partial t^2},$$

where

$$I_i = \int_{-h/2}^{h/2} \rho(z) z^i dz, \quad (\mathrm{i} = 0,1,2,3,4,6),$$
$$J_i = I_i - c_1 I_{i+2}, K_2 = I_2 - 2c_1 I_4 + c_1^2 I_6, c_2 = 3c_1, \quad (14)$$

and the coefficients $I_i (i = 0 \div 4,6)$ are noted in Appendix, and

k_1 - Winkler foundation modulus

k_2 - Pasternak foundation model

q - an external pressure uniformly distributed on the surface of the plate

ε - damping coefficient.

The stress function $f(x,y,t)$ is introduced as

$$N_x = \frac{\partial^2 f}{\partial y^2}, N_y = \frac{\partial^2 f}{\partial x^2}, N_{xy} = -\frac{\partial^2 f}{\partial x \partial y}. \tag{15}$$

Replacing Eq. (15) into the two first Eqs. (13) yields

$$\frac{\partial^2 u}{\partial t^2} = -\frac{J_1}{I_0}\frac{\partial^2 \phi_x}{\partial t^2} + \frac{c_1 I_3}{I_0}\frac{\partial^3 \mathrm{w}}{\partial x \partial t^2}, \tag{16a}$$

$$\frac{\partial^2 v}{\partial t^2} = -\frac{J_1}{I_0}\frac{\partial^2 \phi_y}{\partial t^2} + \frac{c_1 I_3}{I_0}\frac{\partial^3 \mathrm{w}}{\partial y \partial t^2}. \tag{16b}$$

By substituting Eqs. (16) into the Eqs. (13) and Eqs. (13) can be rewritten

$$\begin{aligned}
&\frac{\partial Q_x}{\partial x} + \frac{\partial Q_y}{\partial y} - c_2\left(\frac{\partial R_x}{\partial x} + \frac{\partial R_y}{\partial y}\right) + N_x\frac{\partial^2 \mathrm{w}}{\partial x^2} + 2N_{xy}\frac{\partial^2 \mathrm{w}}{\partial x \partial y} + N_y\frac{\partial^2 \mathrm{w}}{\partial y^2} \\
&+c_1\left(\frac{\partial^2 P_x}{\partial x^2} + 2\frac{\partial^2 P_{xy}}{\partial x \partial y} + \frac{\partial^2 P_y}{\partial y^2}\right) - k_1 \mathrm{w} + k_2\left(\frac{\partial^2 \mathrm{w}}{\partial x^2} + \frac{\partial^2 \mathrm{w}}{\partial y^2}\right) + \frac{N_y}{R} + q \\
&= I_0\frac{\partial^2 \mathrm{w}}{\partial t^2} + 2\varepsilon I_0\frac{\partial \mathrm{w}}{\partial t} + \left(\frac{c_1^2 I_3^2}{I_0} - c_1^2 I_6\right)\left(\frac{\partial^4 \mathrm{w}}{\partial x^2 \partial t^2} + \frac{\partial^4 \mathrm{w}}{\partial y^2 \partial t^2}\right) + \\
&\left(J_4 c_1 - \frac{J_1 I_3 c_1}{I_0}\right)\frac{\partial^3 \phi_x}{\partial x \partial t^2} + \left(J_4 c_1 - \frac{J_1 I_3 c_1}{I_0}\right)\frac{\partial^3 \phi_y}{\partial y \partial t^2},
\end{aligned} \tag{17a}$$

$$\frac{\partial M_x}{\partial x} + \frac{\partial M_{xy}}{\partial y} - c_1\left(\frac{\partial P_x}{\partial x} + \frac{\partial P_{xy}}{\partial y}\right) - Q_x - c_2 R_x = \left(K_2 - \frac{J_1^2}{I_0}\right)\frac{\partial^2 \phi_x}{\partial t^2} + \left(\frac{c_1 I_3 J_1}{I_0} - c_1 J_4\right)\frac{\partial^3 \mathrm{w}}{\partial x \partial t^2}, \tag{17b}$$

$$\frac{\partial M_{xy}}{\partial x} + \frac{\partial M_y}{\partial y} - c_1\left(\frac{\partial P_{xy}}{\partial x} + \frac{\partial P_y}{\partial y}\right) - Q_y - c_2 R_y = \left(K_2 - \frac{J_1^2}{I_0}\right)\frac{\partial^2 \phi_y}{\partial t^2} + \left(\frac{c_1 I_3 J_1}{I_0} - c_1 J_4\right)\frac{\partial^3 \mathrm{w}}{\partial y \partial t^2}. \tag{17c}$$

Substituting Eqs. (12) and (15) into the equation (7), we have:

$$\frac{1}{E_1}\left(\frac{\partial^4 f}{\partial x^4} + 2\frac{\partial^4 f}{\partial x^2 \partial y^2} + \frac{\partial^4 f}{\partial y^4}\right) = \left(\frac{\partial^2 \mathrm{w}}{\partial x \partial y}\right)^2 - \frac{\partial^2 \mathrm{w}}{\partial x^2}\frac{\partial^2 \mathrm{w}}{\partial y^2}. \tag{18}$$

The system of motion Eqs. (17) is rewritten as Eq.(19) by replacing Eq. (6) into Eq. (10) and then into Eqs. (17):

$$\begin{aligned}
&L_{11}(\mathrm{w}) + L_{12}(\phi_x) + L_{13}(\phi_y) + P(\mathrm{w}, f) + q = I_0\frac{\partial^2 \mathrm{w}}{\partial t^2} + 2\varepsilon I_0\frac{\partial \mathrm{w}}{\partial t} \\
&+\left(\frac{c_1^2 I_3^2}{I_0} - c_1^2 I_6\right)\left(\frac{\partial^4 \mathrm{w}}{\partial x^2 \partial t^2} + \frac{\partial^4 \mathrm{w}}{\partial y^2 \partial t^2}\right) + \left(J_4 c_1 - \frac{J_1 I_3 c_1}{I_0}\right)\frac{\partial^3 \phi_x}{\partial x \partial t^2} + \left(J_4 c_1 - \frac{J_1 I_3 c_1}{I_0}\right)\frac{\partial^3 \phi_y}{\partial y \partial t^2},
\end{aligned} \tag{19a}$$

$$L_{21}(\mathrm{w}) + L_{22}(\phi_x) + L_{23}(\phi_y) = \left(K_2 - \frac{J_1^2}{I_0}\right)\frac{\partial^2 \phi_x}{\partial t^2} + \left(\frac{c_1 I_3 J_1}{I_0} - c_1 J_4\right)\frac{\partial^3 \mathrm{w}}{\partial x \partial t^2}, \tag{19b}$$

$$L_{31}(\mathrm{w})+L_{32}(\phi_x)+L_{33}(\phi_y)=\left(K_2-\frac{J_1^2}{I_0}\right)\frac{\partial^2\phi_y}{\partial t^2}+\left(\frac{c_1I_3J_1}{I_0}-c_1J_4\right)\frac{\partial^3\mathrm{w}}{\partial y\partial t^2}, \tag{19c}$$

and the $L_{ij}(i=1-3, j=1-3)$ and P are noted in Appendix.

In next section, in order to determined nonlinear dynamical analysis of PFGCP using the third order shear deformation theory, the Eqs. (18)-(19) are used along with boundary conditions and initial conditions

2.2. Boundary conditions

In order to determined nonlinear dynamical analysis of PFGCP, the edges of the PFGCP are simply supported and immovable (IM) and boundary conditions are [27, 28]:

$$\begin{aligned}&\mathrm{w}=u=\phi_y=M_x=P_x=0,\quad N_x=N_{x0}\ \ at\ \ x=0,\,a,\\&\mathrm{w}=v=\phi_x=M_y=P_x=0,\quad N_y=N_{y0}\ \ at\ \ y=0,\,b,\end{aligned} \tag{20}$$

in which N_{x0}, N_{y0} are forces along the *x* and *y* axis.

Wiht the boundary condition (20) and In order to solve Eqs. (18) and (19), the approximate solutions can be written as [26]:

$$\begin{aligned}&\mathrm{w}(x,y,t)=\mathrm{W}(t)\sin\alpha x\sin\beta y,\\&\phi_x(x,y,t)=\Phi_x(t)\cos\alpha x\sin\beta y,\\&\phi_y(x,y,t)=\Phi_y(t)\sin\alpha x\cos\beta y,\end{aligned} \tag{21}$$

with

$\alpha=\frac{m\pi}{a}, \beta=\frac{n\pi}{b}$ and $m,n=1,2,...$ are the numbers of half waves in the direction x, y, W, Φ_x, Φ_y - the amplitudes which are functions dependent on time.

The stress function is defined as:

$$f(x,y,t)=A_1(t)\cos 2\alpha x+A_2(t)\cos 2\beta y+\frac{1}{2}N_{x0}y^2+\frac{1}{2}N_{y0}x^2, \tag{22a}$$

with

$$A_1=\frac{E_1\beta^2}{32\alpha^2}W^2; A_2=\frac{E_1\alpha^2}{32\beta^2}W^2. \tag{22b}$$

2.3. Nonlinear dynamical analysis

In ordet to obtain Eqs. (23), Eqs. (21) and (22) are replaced into the Eq. (19) after that applying Galerkin method:

$$\begin{aligned}&\left[l_{11}-\left(N_{x0}\alpha^2+N_{y0}\beta^2\right)\right]W+l_{12}\Phi_x+l_{13}\Phi_y+n_1W^3+\frac{16}{mn\pi^2}q=n_2\frac{\partial^2\mathrm{W}}{\partial t^2}+2\varepsilon I_0\frac{\partial\mathrm{W}}{\partial t}\\&+\rho_2\frac{m\pi}{a}\frac{\partial^2\Phi_x}{\partial t^2}+\rho_2\frac{n\pi}{b}\frac{\partial^2\Phi_y}{\partial t^2},\end{aligned} \tag{23a}$$

$$l_{21}W+l_{22}\Phi_x+l_{23}\Phi_y=\rho_1\frac{\partial^2\Phi_x}{\partial t^2}+\rho_2\frac{m\pi}{a}\frac{\partial^2\mathrm{W}}{\partial t^2}, \tag{23b}$$

$$l_{31}\mathrm{W}+l_{32}\Phi_x+l_{33}\Phi_y=\rho_1\frac{\partial^2\Phi_y}{\partial t^2}+\rho_2\frac{n\pi}{b}\frac{\partial^2\mathrm{W}}{\partial t^2}, \tag{23c}$$

Where $\rho_1=K_2-\frac{J_1^2}{I_0};\rho_2=\frac{c_1I_3J_1}{I_0}-c_1J_4$,

$$l_{11}=-\frac{1}{2(1+\nu)}\left[E_1-3c_1E_3-c_2\left(E_3-3c_1E_5\right)\right]\left(\left(\frac{m\pi}{a}\right)^2+\left(\frac{n\pi}{b}\right)^2\right)$$

$$-\frac{c_1^2}{1-\nu^2}\left(\left(\frac{m\pi}{a}\right)^2+\left(\frac{n\pi}{b}\right)^2\right)^2\left(E_7-\frac{E_4^2}{E_1}\right)-k_1-k_2\left(\left(\frac{m\pi}{a}\right)^2+\left(\frac{n\pi}{b}\right)^2\right)+\left(\frac{m\pi}{a}\right)^2\frac{1}{R},$$

$$l_{12}=-\frac{1}{2(1+\nu)}\frac{m\pi}{a}\left[E_1-3c_1E_3-c_2\left(E_3-3c_1E_5\right)\right]+\frac{c_1}{1-\nu^2}\left(\frac{m\pi}{a}\right)^3\left[E_5-\frac{E_2E_4}{E_1}-c_1\left(E_7-\frac{E_4^2}{E_1}\right)\right]$$

$$+c_1\left[\left(\frac{1}{1+\nu}+\frac{\nu}{1-\nu^2}\right)\left(E_5-\frac{E_2E_4}{E_1}\right)-c_1\left(\frac{\nu}{1-\nu^2}+\frac{1}{1+\nu}\right)\left(E_7-\frac{E_4^2}{E_1}\right)\right]\frac{m\pi}{a}\left(\frac{n\pi}{b}\right)^2,$$

$$l_{13}=-\frac{1}{2(1+\nu)}\frac{n\pi}{b}\left[E_1-3c_1E_3-c_2\left(E_3-3c_1E_5\right)\right]+\frac{c_1}{1-\nu^2}\left(\frac{n\pi}{b}\right)^3\left[E_5-\frac{E_2E_4}{E_1}-c_1\left(E_7-\frac{E_4^2}{E_1}\right)\right]$$

$$+c_1\left[\left(\frac{1}{1+\nu}+\frac{\nu}{1-\nu^2}\right)\left(E_5-\frac{E_2E_4}{E_1}\right)-c_1\left(\frac{\nu}{1-\nu^2}+\frac{1}{1+\nu}\right)\left(E_7-\frac{E_4^2}{E_1}\right)\right]\left(\frac{m\pi}{a}\right)^2\frac{n\pi}{b},$$

$$n_1=-\frac{E_1}{16}\left(\left(\frac{m\pi}{a}\right)^4+\left(\frac{n\pi}{b}\right)^4\right),$$

$$n_2=I_0+c_1^2\left(I_6-\frac{I_3^2}{I_0}\right)\left(\left(\frac{m\pi}{a}\right)^2+\left(\frac{n\pi}{b}\right)^2\right),$$

$$l_{21}=-\frac{c_1}{1-\nu^2}\frac{m\pi}{a}\left(\left(\frac{m\pi}{a}\right)^2+\left(\frac{n\pi}{b}\right)^2\right)\left(c_1E_7-\frac{c_1E_4^2}{E_1}-E_5+\frac{E_2E_4}{E_1}\right)$$

$$-\frac{1}{2(1+\nu)}\frac{m\pi}{a}\left[\left(E_1-3c_1E_3\right)+c_2\left(E_3-3c_1E_5\right)\right],$$

$$l_{22}=-\left(\frac{1}{1-\nu^2}\left(\frac{m\pi}{a}\right)^2+\frac{1}{2(1+\nu)}\left(\frac{n\pi}{b}\right)^2\right)\left[E_3-\frac{E_2^2}{E_1}-2c_1\left(E_5-\frac{E_2E_4}{E_1}\right)+c_1^2\left(E_7-\frac{E_4^2}{E_1}\right)\right]$$

$$-\frac{1}{2(1+\nu)}\left[\left(E_1-3c_1E_3\right)+c_2\left(E_3-3c_1E_5\right)\right],$$

$$l_{23}=-\frac{1}{2(1-\nu)}\frac{mn\pi^2}{ab}\left[E_3-\frac{E_2^2}{E_1}-2c_1\left(E_5-\frac{E_2E_4}{E_1}\right)+c_1^2\left(E_7-\frac{E_4^2}{E_1}\right)\right],$$

$$l_{31}=-\frac{c_1}{1-\nu^2}\frac{n\pi}{b}\left[c_1E_7-c_1\frac{E_4^2}{E_1}-E_5+\frac{E_2E_4}{E_1}\right]\left(\left(\frac{m\pi}{a}\right)^2+\left(\frac{n\pi}{b}\right)^2\right)-\frac{1}{2(1+\nu)}\frac{n\pi}{b}\left[E_1-3c_1E_3+c_2\left(E_3-3c_1E_5\right)\right],$$

$$l_{32}=-\frac{1}{2(1-\nu)}\frac{mn\pi^2}{ab}\left[E_3-\frac{E_2^2}{E_1}-2c_1\left(E_5-\frac{E_2E_4}{E_1}\right)+c_1^2\left(E_7-\frac{E_4^2}{E_1}\right)\right],$$

$$l_{33}=-\left(\frac{1}{1-\nu^2}\left(\frac{n\pi}{b}\right)^2+\frac{1}{2(1+\nu)}\left(\frac{m\pi}{a}\right)^2\right)\left[E_3-\frac{E_2^2}{E_1}-2c_1\left(E_5-\frac{E_2E_4}{E_1}\right)+c_1^2\left(E_7-\frac{E_4^2}{E_1}\right)\right]$$

$$-\frac{1}{2(1+\nu)}\left[E_1-3c_1E_3+c_2\left(E_3-3c_1E_5\right)\right],$$

In order to investigate the effect of thermal load on the PFGCP. The modeling are simply supported and immovable in all edges. In other words, boundary conditions of case stud is $u=0$ (on $x=0,a$) and $\mathrm{v}=0$ (on $y=0,b$), and and is satisfied equations as [10, 29]:

$$\int_0^b\int_0^a\frac{\partial u}{\partial x}dxdy=0,\ \int_0^a\int_0^b\frac{\partial v}{\partial y}dxdy=0. \tag{24}$$

With Eqs. (6) and (12) along with (15), Ep (25) is determined as:

$$\begin{aligned}\frac{\partial u}{\partial x}&=\frac{1}{E_1}\left(f_{,yy}-\nu f_{,xx}\right)-\frac{E_2}{E_1}\phi_{x,x}+\frac{c_1E_4}{E_1}\left(\phi_{x,x}+w_{,xx}\right)-\frac{w}{R}-\frac{1}{2}\left(\frac{\partial w}{\partial x}\right)^2+\frac{\Phi_a}{E_1},\\ \frac{\partial v}{\partial y}&=\frac{1}{E_1}\left(f_{,xx}-\nu f_{,yy}\right)-\frac{E_2}{E_1}\phi_{y,y}+\frac{c_1E_4}{E_1}\left(\phi_{y,y}+w_{,yy}\right)-\frac{1}{2}\left(\frac{\partial w}{\partial y}\right)^2+\frac{\Phi_a}{E_1}.\end{aligned} \tag{25}$$

In order to obtain Eqs. (26), Eqs. (21) and (22) are placed into Eq. (25) then the obtained result are replaced into Eq. (24) we have:

$$N_{x0}=-\frac{\Phi_a}{1-\nu}-\frac{4}{mn\pi^2\left(1-\nu^2\right)}\left[\left(E_2-c_1E_4\right)\left(\alpha\Phi_x+\nu\beta\Phi_y\right)-c_1E_4\left(\alpha^2+\nu\beta^2\right)W\right]$$

$$+\frac{E_1}{8\left(1-\nu^2\right)}\left(\alpha^2+\nu\beta^2\right)W^2, \tag{26a}$$

$$N_{y0}=-\frac{\Phi_a}{1-\nu}-\frac{4}{mn\pi^2\left(1-\nu^2\right)}\left[\left(E_2-c_1E_4\right)\left(\nu\alpha\Phi_x+\beta\Phi_y\right)-c_1E_4\left(\nu\alpha^2+\beta^2\right)W\right]$$

$$+\frac{E_1}{8\left(1-\nu^2\right)}\left(\nu\alpha^2+\beta^2\right)W^2. \tag{26b}$$

Putting Eqs. (26) into the Eq. (23). We obtain:

$$\left[l_{11}+\left(\left(\frac{m\rho}{a}\right)^2+\left(\frac{n\rho}{b}\right)^2\right)\frac{\mathrm{F}_a}{1-\nu}\right]W+l_{12}\mathrm{F}_x+l_{13}\mathrm{F}_y+l_{14}\mathrm{F}_x\mathrm{W}+l_{15}\mathrm{F}_y\mathrm{W}+l_{16}W^2+l_{17}W^3$$

$$+\frac{16}{mn\rho^2}q=n_2\frac{\P^2\mathrm{W}}{\P t^2}+2eI_0\frac{\P\mathrm{W}}{\P t}+r_2\frac{m\rho}{a}\frac{\P^2\mathrm{F}_x}{\P t^2}+r_2\frac{n\rho}{b}\frac{\P^2\mathrm{F}_y}{\P t^2}, \tag{27a}$$

$$l_{21}W+l_{22}\Phi_x+l_{23}\Phi_y=\rho_1\frac{\partial^2\Phi_x}{\partial t^2}+\rho_2\frac{m\pi}{a}\frac{\partial^2\mathrm{W}}{\partial t^2}, \tag{27b}$$

$$l_{31}\mathrm{W}+l_{32}\Phi_x+l_{33}\Phi_y=\rho_1\frac{\partial^2\Phi_y}{\partial t^2}+\rho_2\frac{n\pi}{b}\frac{\partial^2\mathrm{W}}{\partial t^2}, \tag{27c}$$

with

$$l_{14}=\frac{4\left(E_2-c_1E_4\right)\left(\left(\frac{m\pi}{a}\right)^2+v\left(\frac{n\pi}{b}\right)^2\right)}{mn\pi^2\left(1-v^2\right)}\frac{m\pi}{a},$$

$$l_{15}=\frac{4\left(E_2-c_1E_4\right)\left(\left(\frac{m\pi}{a}\right)^2v+\left(\frac{n\pi}{b}\right)^2\right)}{mn\pi^2\left(1-v^2\right)}\frac{n\pi}{b},$$

$$l_{16}=-\frac{4c_1E_4\left(\alpha^4+2v\alpha^2\beta^2+\beta^4\right)}{mn\pi^2\left(1-v^2\right)},$$

$$l_{17}=n_1-\frac{E_1}{8\left(1-v^2\right)}\left[\left(\frac{m\pi}{a}\right)^4+2v\left(\frac{m\pi}{a}\right)^2\left(\frac{n\pi}{b}\right)^2+\left(\frac{n\pi}{b}\right)^4\right],$$

The Eqs. (27) are used to dertermine dynamic analysis of PFGCP with suported by elastic foundations along with the effect of temperature with the appearance of the coefficient Φ_a.

In order to obtain the natural frequencies (ω) of PFGCP, solving determinant of matrix (28) with linear coefficients taken from Eqs. (27) along with $q=0$. The obtained results are three natural frequencies, the smallest value will be selected.

$$\begin{vmatrix} l_{11}+\left(\left(\frac{m\pi}{a}\right)^2+\left(\frac{n\pi}{b}\right)^2\right)\frac{\Phi_a}{1-v}+n_2\omega^2 & l_{12}+\rho_2\frac{m\pi}{a}\omega^2 & l_{13}+\rho_2\frac{n\pi}{b}\omega^2 \\ l_{21}+\rho_2\frac{m\pi}{a}\omega^2 & l_{22}+\rho_1\omega^2 & l_{23} \\ l_{31}+\rho_2\frac{n\pi}{b}\omega^2 & l_{32} & l_{33}+\rho_1\omega^2 \end{vmatrix}=0. \tag{28}$$

3. Numerical results and discussion

In this paper, consider PFGCP is under the influence of a uniformly distributed load on the surface with equations in the harmonic function $q=Q\sin\Omega t$ with Q is the amplitude of uniformly excited load. Besides, the fourth-order Runge-Kutta method is used to solve equations (27) and the material properties of the component material are given as [40]:

$E_c=380\times10^9\,N/m^2,\rho_c=3800kg/m^3,\alpha_c=7.4\times10^{-6o}C^{-1},K_c=10.4W/mK,$

$E_m=70\times10^9\,N/m^2,\rho_m=2702kg/m^3,\alpha_m=23\times10^{-6o}C^{-1},K_m=204W/mK,$

$v=0.3,$

3.1. Natural frequency

In order to verify the reliability of the used method, the numerical results of this paper will be compared with the published results of Duc et al [40]. In the Duc author's paper, the used method is high order shear deformation for FGM plate. In order to obtain the highest accuracy of the comparison results, the modeling of this paper was brought to the same format as the modeling in Duc's paper by R = infinity. The comparison results of the free natural frequency are shown in Table 1. It can be seen that the results of both papers are not much different. It verifies that the used method is reliable.

Table 1. Comparison of natural frequency $\left(s^{-1}\right)$ of PFGCP with other paper with same conditions as $a/b=1, a/h=20, N=1$.

$(k_1;k_2)$ $(GPa/m;GPa.m)$	$\Delta T\left(^oC\right)$	Natural frequency $\left(s^{-1}\right)$	
		Duc et al [40]	Present study
$(0;0)$	0	1941.73	1922
	50	1570.25	1522
	105	1015.19	1082
$(0.25;0)$	0	2303.00	2341
	50	1999.79	1998
	105	1601.28	1687
$(0.25;0.02)$	0	2779.46	2790
	50	2533.92	2576
	105	2232.86	2293

The natural frequencies $\left(s^{-1}\right)$ of PFGCP with the influence of index N, modes (m,n) along with $a/b=1, a/h=20, k_1=0, k_2=0$, $\Delta T=100^oC$ and using type 2 of porosity distribution. We can see that the natural frequencies will raise when modes (m,n) increase in which index N is constant. In contrast, when index N increase in which modes (m,n) is constant, the natural frequencies increase. Form equation (1), it can be explained that index $N = 0$ corresponding to isotropic uniform panel is made from ceramic materials, $N = 1$ is the case when the ceramic and metal components are distributed linearly over the thickness of the structure wall and when N increase, the volume ratio of the metal component in the structure increases.

Table 2. The natural frequencies $\left(s^{-1}\right)$ of PFGCP with the influnece of index N, modes (m,n) along with $a/b=1, a/h=20, k_1=0, k_2=0, R/h=400$ and $\Delta T=100^oC$.

N	ω_1 $(m=1,n=1)$	ω_2 $(m=1,n=3)$	ω_3 $(m=1,n=5)$	ω_4 $(m=3,n=5)$	ω_5 $(m=5,n=5)$
0.5	2702	11175	27051	34564	48871
1	2434	9766	24060	30838	43767
3	2251	8817	21037	26808	37785
5	2172	8505	20218	25719	36137
12	2080	8174	19369	24594	34440
∞	1629	6195	14636	18610	26149

Table 3 shows the natural frequencies $\left(s^{-1}\right)$ of PFGCP with the influnece of ratio a/b, elastic foundation, porosity distribution type along with $a/h=20, N=1, \Delta T=100^{o}C$, $(m,n)=(1,1), R/h=400$. It can easily see that the natural frequencies increase when ratio a/b raises as well as when modeling is supported by elastic foundations. Furthermore, the comparison of the effect between type 1 of porosity distribution and type 2 of porosity distribution are shown in table 3. The effect of type 2 of porosity distribution on the natural frequencies is smaller than the effect type 1 of porosity distribution.

Table 3. The natural frequencies $\left(s^{-1}\right)$ of PFGCP with the influnece of ratio a/b, elastic foundation $(m,n)=(1,1), R/h=400 \;\; a/h=20, N=1, \Delta T=100^{o}C.$

$(k_1;k_2)$ $(GPa/m;GPa.m)$	a/b	Natural frequency $\left(s^{-1}\right)$	
		Type 1	Typ 2
$(0;0)$	1	2525	2434
	1.5	3757	3393
	2	5448	5068
$(0.2;0)$	1	2757	2449
	1.5	3917	3569
	2	5559	5187
$(0.2;0.04)$	1	3528	3292
	1.5	4816	4538
	2	6554	6242

3.2. Nonlinear dynamic response

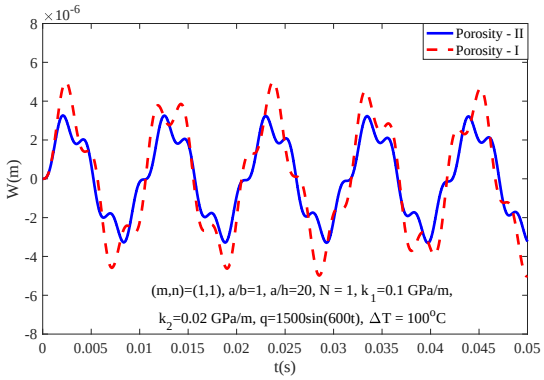

Fig. 2. Comparision between two type of porosity distribution in PFGCP.

Figure 2 shows the effect of porosity distribution on nonlinear dynamic response of the PFGCP with $a/b=1, a/h=20, \Delta T=0, \varepsilon=0.1$. It can easily see that the amplitude of deflection for PFGCP in case Porosity I bigger more than the amplitude of deflection for PFGCP in Porosity II. In other words, the porosity distribition Porosity II will enhance the loading carrying capacity of PFGCP more than the Porosity I. Thus, other results will use the Porosity II to investigate the effect of other factors on the nonlinear dynamic response of the panel.

Figures 3 and 4 give the nonlinear dynamic response of PFGCP with the influence of ratio a/b, ratio a/h and supported by elastic foundations. The amplitude of deflection of the PFGCP will raise when increasing ratio a/h or decrease a/b. In figure 3, the amplitude of deflection has the highest value with $a/b=1$. When increasing a/b from 1 to 2, the amplitude of deflection decreases about 7 times. In figure 4, the amplitude of deflection has the smallest value with $a/h=40$. When increasing a/h from 20 to 40, the amplitude of deflection raise about 9 times.

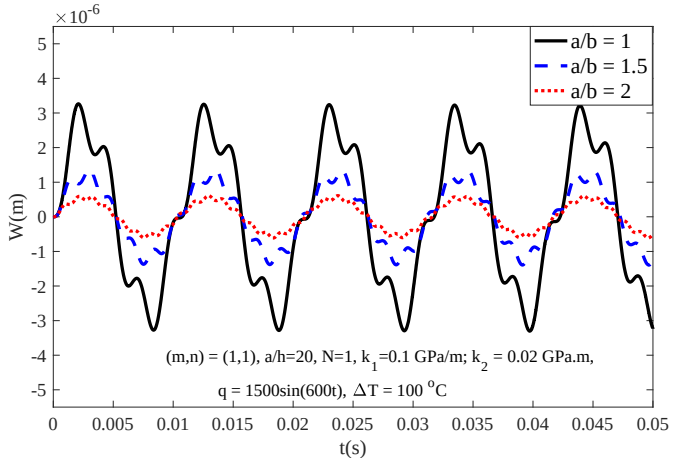

Fig. 3. The nonlinear dynamical response of the PFGCP with influence of effect of ratio a/b.

The influence of index N on the nonlinear dynamic response of the PFGCP is investigated in figure 5. From figure 5 can see that the amplitude vibration of the PFGCP will raise when the index N increase and change about 2.3 times. This behavior can be explained that the index N increase results in a volume ratio of ceramic more bigger than a volume ratio of metal. It leads to bigger change in Elastic modulus, in other words, it leads to decrease load carrying capacity of the PFGCP.

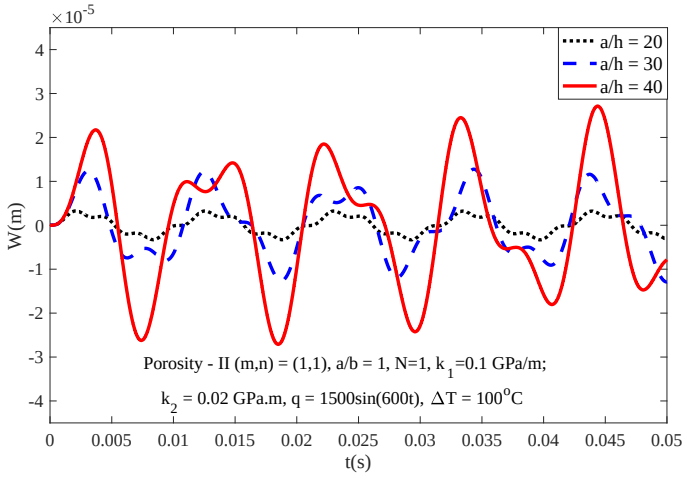

Fig. 4. The nonlinear dynamical response of the PFGCP with influence of effect of ratio a/h.

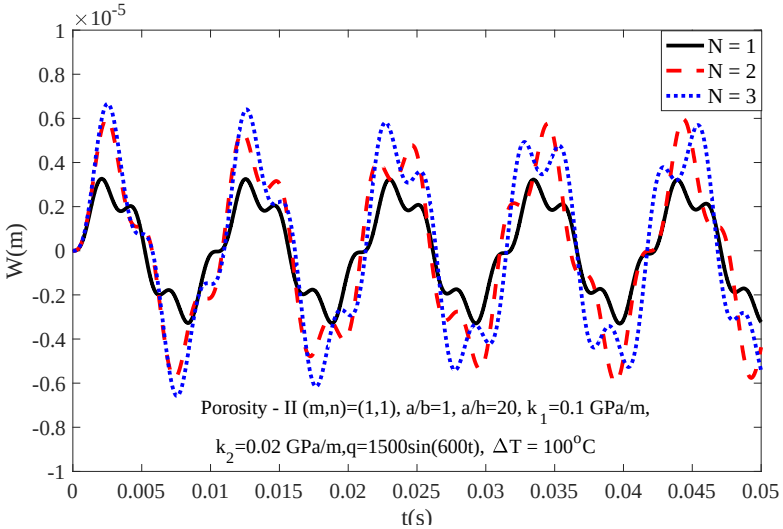

Fig. 5. Effect of power law index N on nonlinear dynamical response of the PFGCP.

The influence of elastic foundations on the nonlinear dynamic response of the PFGCP with $a/b=1,\ a/h=20, N=1, \Delta T=100^{o}C$ are shown in figures 6 and 7. It clear that the elastic foundations: Winkler foundation (figure 6) and Pasternak foundations (figure 7) has a positive influence on the amplitude vibrations. When increasing the Winkler foundation, the Pasternak foundations, the amplitude vibrations will decrease. But the influence of the Pasternak foundation better than Winkler foundations, the amplitude vibrations will enhance about 200% with the change of the Winkler foundation in which the amplitude vibrations will enhance about 250%. In order to enhance the load carrying capacity of modeling, the elastic foundations have an important role.

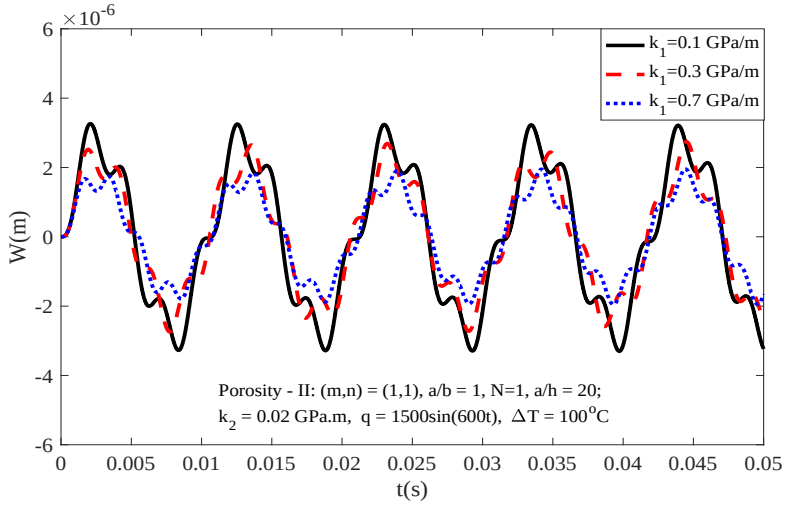

Fig. 6. Effect of the linear Winkler foundation on nonlinear dynamical response of the PFGCP.

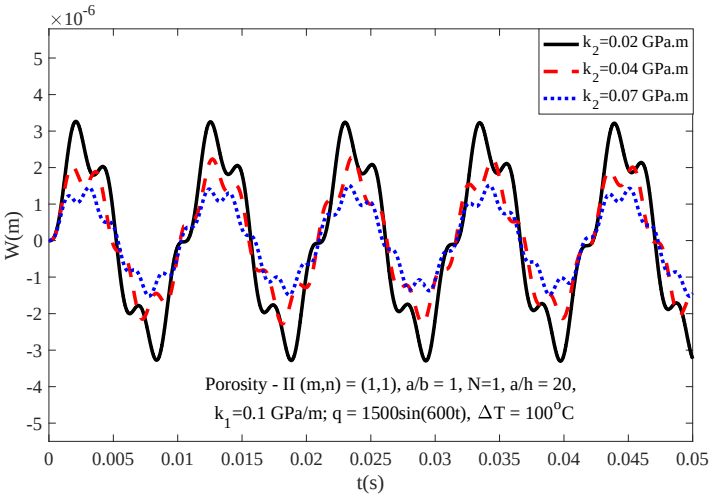

Fig. 7. Effect of the Pasternak foundation on nonlinear dynamical response of the PFGCP.

The influence of exciting force amplitude on nonlinear dynamic response of the PFGCP with $Q=\left(1500,1800,2500\,N/m^2\right)$ and $\Delta T=100^oC$ are proposed in figure 8. The amplitude of vibration will raise when the excited force amplitude increase. In other words, the exciting force amplitude decrease, the amplitude of vibration will decrease.

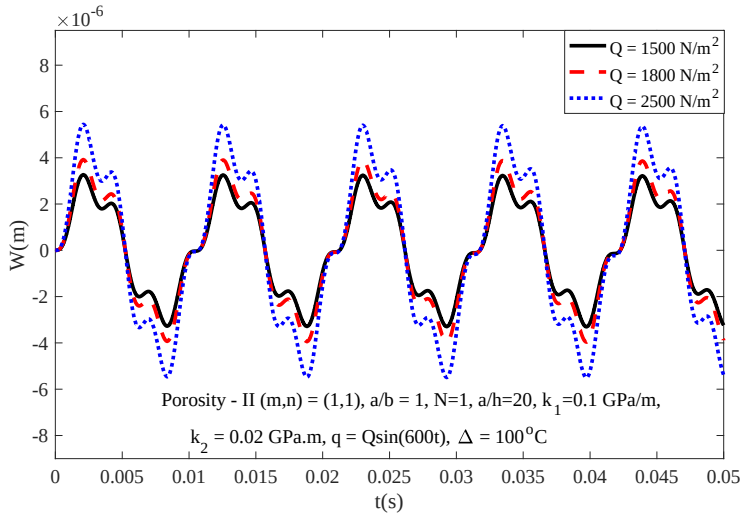

Fig. 8. Nonlinear dynamic responses of the PFGCP with different loads.

The nonlinear response of the PFGCP with the effect of uniform temperature is presented in figure 9. From figure 9, it can easily seen that the uniform temperature has a negative influence on the amplitude deflection of the cylindrical panel PFG. The amplitude deflection of the PFGCP will increase when the uniform temperature rise. It can be explained that the uniform temperature changes the stiffness matrix.

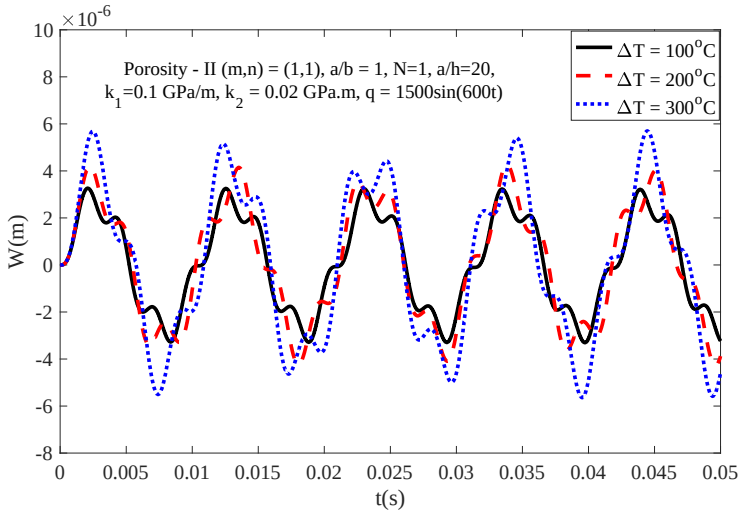

Fig. 9. Effect of uniform temperature rise on nonlinear response of the PFGCP.

4. Conclusions

This is the first paper uses the high order shear deformation theory and Ahry function to investigate the nonlinear dynamic response and vibration of panel FGM with porosity distribution. Besides, the PFGCP is supported by elastic foundations and under mechanical load, thermal load. By using the Galerkin method as well as the four-order Runge-Kutta method, the numerical results for nonlinear dynamic response of modelings are described by figure and table with the influences of the materials properties, thermal load, mechanical load, elastic foundations, geometrical parameters, the porosity distribution type. This paper obtained some remarkable results as:

- The porosity distribution type 2 will enhance the loading carrying capacity of PFGCP more than the porosity distribution type 1.

- The amplitude of deflection of the PFGCP will raise when increasing ratio a/h or decrease a/b.

- The amplitude vibration of the PFGCP will raise when the index N increase and changes about 2.3 times.

- When increasing the Winkler foundation, the Pasternak foundations, the amplitude vibrations will decrease. The influence of the Pasternak foundation better than Winkler foundations.

- The amplitude of vibration will raise when the exciting force amplitude increase.

- The uniform temperature has a negative influence on the amplitude deflection of the cylindrical panel PFG. The amplitude deflection of the PFGCP will increase when the uniform temperature rise.

Acknowledgements

This work has been supported by VNU Hanoi - University of Engineering and Technology under the project number CN.19.04. The authors are grateful to this support.

References

[1] X.W. Chen, Z.Q. Yue, Contact mechanics of two elastic spheres reinforced by functionally graded materials (FGM) thin coatings**,** Engineering Analysis with Boundary Elements 109 (2019) 57-69.

[2] Z. Li, J. Zheng, Q. Sun, H. He, Nonlinear structural stability performance of pressurized thin-walled FGM arches under temperature variation field, International Journal of Non-Linear Mechanics 113 (2019) 86 – 102.

[3] S. Dastjerdi, B. Akgöz, New static and dynamic analyses of macro and nano FGM plates using exact three-dimensional elasticity in thermal environment, Composite Structures 192 (2018) 626-641.

[4] Y.Q. Wang, W.Z. Jean, Nonlinear dynamic thermoelastic response of rectangular FGM plates with longitudinal velocity, Composites Part B: Engineering 117 (2017) 74-88.

[5] A.H. Sofiyev, Dynamic response of an FGM cylindrical shell under moving loads, Composite Structures 93 (2010) 58-66.

[6] Z.X. Wang, H.S. Shen, Nonlinear dynamic response of sandwich plates with FGM face sheets resting on elastic foundations in thermal environments, Ocean Engineering 57 (2013) 99-110.

[7] M. Shariyat, Vibration and dynamic buckling control of imperfect hybrid FGM plates with temperature-dependent material properties subjected to thermo-electro-mechanical loading conditions, Composite Structures 88 (2009) 240-252.

[8] S.J. Singh, S.P. Harsha, Nonlinear dynamic analysis of sandwich S- FGM plate resting on pasternak foundation under thermal environment, European Journal of Mechanics - A/Solids 76 (2019) 155-179.

[9] K. Gao, W. Gao, D. Wu, C. Song, Nonlinear dynamic buckling of the imperfect orthotropic E- FGM circular cylindrical shells subjected to the longitudinal constant velocity, International Journal of Mechanical Sciences 138–139 (2018) 199-209.

[10] J. N. Reddy, C.D. Chin, Thermo-mechanical analysis of functionally graded cylinders and plates, J. Thermal Stress; 21 (1998) 593-626.

[11] H. Babaei, Y. Kiani, M.R. Eslami, Thermal buckling and post-buckling analysis of geometrically imperfect FGM clamped tubes on nonlinear elastic foundation, Applied Mathematical Modelling 71 (2019) 12-30.

[12] S.C. Han, W.T. Park, W.Y. Jung, 3D graphical dynamic responses of FGM plates on Pasternak elastic foundation based on quasi-3D shear and normal deformation theory, Composites Part B: Engineering 95 (2016) 324-334.

[13] S.E. Ghiasian, Y. Kiani, M.R. Eslami, Dynamic buckling of suddenly heated or compressed FGM beams resting on nonlinear elastic foundation, Composite Structures 106 (2013) 225-234.

[14] M. Javani, Y. Kiani and M.R. Eslami, Geometrically nonlinear rapid surface heating of temperature-dependent FGM arches, Aerospace Science and Technology 90 (2019) 264-274.

[15] M. Shariyat, Dynamic thermal buckling of suddenly heated temperature-dependent FGM cylindrical shells, under combined axial compression and external pressure, International Journal of Solids and Structures 45 (2008) 2598-2612.

[16] H. Babaei, Y. Kiani, M.Z. Eslami, Large amplitude free vibration analysis of shear deformable FGM shallow arches on nonlinear elastic foundation, Thin-Walled Structures 144 (2019) 106237.

[17] K. Gao, R. Li and J. Yang, Dynamic characteristics of functionally graded porous beams with interval material properties, Engineering Structures 197 (2019) 109441.

[18] H. Yang, X. Hao, J. Tang, W. Jin, J. Hu, Dual-functional porous copper films modulated via dynamic hydrogen bubble template for in situ SERS monitoring electrocatalytic reaction. Applied Surface Science 494 (2019) 731-739.

[19] K. Foroutan, A. Shaterzadeh, H. Ahmadi, Nonlinear static and dynamic hygrothermal buckling analysis of imperfect functionally graded porous cylindrical shells, Applied Mathematical Modelling January 77 (2020) 539-553.

[20] Q. Li, D. Wu, X. Chen, L. Liu, W. Gao, Nonlinear vibration and dynamic buckling analyses of sandwich functionally graded porous plate with graphene platelet reinforcement resting on Winkler–Pasternak elastic foundation, International Journal of Mechanical Sciences 148 (2018) 596-610.

[21] H.N. Li, P.F. Liu, C. Li, G. Li, H. Zhang, Experimental research on dynamic mechanical properties of metal tailings porous concrete, Construction and Building Materials 213 (2019) 20-31.

[22] S.S. Mirjavadi, B M. Afshari, M.R. Barati, A.M.S. Hamouda, Transient response of porous FG nanoplates subjected to various pulse loads based on nonlocal stress-strain gradient theory, European Journal of Mechanics - A/Solids March–April 74 (2019) 210-220.

[23] M. Esmaeilzadeh, M. Kadkhodayan, Dynamic analysis of stiffened bi-directional functionally graded plates with porosities under a moving load by dynamic relaxation method with kinetic damping, Aerospace Science and Technology 93 (2019) 105333.

[24] F. Ebrahimi, A. Jafari, M.R. Barati, Vibration analysis of magneto-electro-elastic heterogeneous porous material plates resting on elastic foundations, Thin-Walled Structures 119 (2017) 33-46.

[25] E. Arshid, A.R. Khorshidvand, Free vibration analysis of saturated porous FG circular plates integrated with piezoelectric actuators via differential quadrature method, Thin-Walled Structures 125 (2018) 220-233.

[26] M.H. Shojaeefard, H.S. Googarchin, M. Ghadiri, M. Mahinzare, Micro temperature-dependent FG porous plate: Free vibration and thermal buckling analysis using modified couple stress theory with CPT and FSDT, Applied Mathematical Modelling 50 (2017) 633-655.

[27] P.A. Demirhan, V. Taskin, Bending and free vibration analysis of Levy-type porous functionally graded plate using state space approach, Composites Part B: Engineering 160 (2019) 661-676.

[28] D.G. Zhang, Nonlinear bending analysis of FGM beams based on physical neutral surface and high order shear deformation theory, Composite Structures 100 (2013) 121-126.

[29] J.N. Reddy, C.D. Chin, Thermo-mechanical analysis of functionally graded cylinders and plates, J. Thermal Stress 21 (1998) 593-626.

[30] D.G. Zhang, Modeling and analysis of FGM rectangular plates based on physical neutral surface and high order shear deformation theory. International Journal of Mechanical Science 68 (2013) 92-104.

[31] A. Thon, P. Bélanger, EMAT design for minimum remnant thickness gauging using high order shear horizontal modes. Ultrasonics 95 (2019) 70-78.

[32] M. Meunier, R.A. Shenoi, Dynamic analysis of composite sandwich plates with damping modelled using high order shear deformation theory. Composite Structures 54 (2001) 243-254.

[33] P.H. Cong, V.M. Anh, N.D. Duc, Nonlinear dynamic response of eccentrically stiffened FGM plate using Reddy's TSDT in thermal environment, Journal of Thermal Stresses 40 (2017) 704-732.

[34] Shufrin, M. Eisenberger, Stability of variable thickness shear deformable plates—first order and high order analyses, Thin-Walled Structures 43 (2005) 189-207.

[35] V. Stojanović, P. Kozić, G Janevski, Exact closed-form solutions for the natural frequencies and stability of elastically connected multiple beam system using Timoshenko and high order shear deformation theory, Journal of Sound and Vibration 332 (2013) 563-576.

[36] O. Attia, A. El-Zafrany, A high order shear element for nonlinear vibration analysis of composite layered plates and shells, International Journal of Mechanical Sciences 41 (1999) 461-486.

[37] N.D. Khoa, V.M. Anh, N.D. Duc, Nonlinear dynamic response and vibration of functionally graded nanocomposite cylindrical panel reinforced by carbon nanotubes in thermal environment, Journal of Sandwich Structures & Materials, 2019. https://doi.org/10.1177/1099636219847191.

[38] E. Allahyari, M. Asgari, Thermo-mechanical vibration of double-layer graphene nanosheets in elastic medium considering surface effects; developing a nonlocal third order shear deformation theory, European Journal of Mechanics - A/Solids 75 (2019) 307-321.

[39] X. Wang, G. Shi, A refined laminated plate theory accounting for the third order shear deformation and interlaminar transverse stress continuity, Applied Mathematical Modelling 39 (2015) 5659-5680.

[40] N.D. Duc, D.H. Bich, P.H. Cong, Nonlieanr thermal dynamic response of shear deformable FGM plates on elastic foundations. Journal of Thermal Stresses 29 (2016) 278 – 297.

Appendix

$$L_{11}(\mathrm{w}) = \frac{1}{2(1+\nu)}\left[E_1 - 3c_1E_3 - c_2\left(E_3 - 3c_1E_5\right)\right]\left(\frac{\partial^2 \mathrm{w}}{\partial x^2} + \frac{\partial^2 \mathrm{w}}{\partial y^2}\right)$$
$$-\frac{c_1^2}{1-\nu^2}\left[\frac{\partial^4 \mathrm{w}}{\partial x^4} + 2\frac{\partial^4 \mathrm{w}}{\partial x^2\partial y^2} + \frac{\partial^4 \mathrm{w}}{\partial y^4}\right]\left(E_7 - \frac{E_4^2}{E_1}\right) - k_1\mathrm{w} + k_2\left(\frac{\partial^2 \mathrm{w}}{\partial x^2} + \frac{\partial^2 \mathrm{w}}{\partial y^2}\right),$$
$$L_{12}(\phi_x) = \frac{1}{2(1+\nu)}\left[E_1 - 3c_1E_3 - c_2\left(E_3 - 3c_1E_5\right)\right]\frac{\partial \phi_x}{\partial x} + \frac{c_1}{1-\nu^2}\left[E_5 - \frac{E_2E_4}{E_1} - c_1\left(E_7 - \frac{E_4^2}{E_1}\right)\right]\frac{\partial^3 \phi_x}{\partial x^3}$$
$$+c_1\left[\left(\frac{1}{1+\nu} + \frac{\nu}{1-\nu^2}\right)\left(E_5 - \frac{E_2E_4}{E_1}\right) - c_1\left(\frac{\nu}{1-\nu^2} + \frac{1}{1+\nu}\right)\left(E_7 - \frac{E_4^2}{E_1}\right)\right]\frac{\partial^3 \phi_x}{\partial x\partial y^2},$$
$$L_{13}(\phi_y)\frac{1}{2(1+\nu)}\left[E_1 - 3c_1E_3 - c_2\left(E_3 - 3c_1E_5\right)\right]\frac{\partial \phi_y}{\partial y} + \frac{c_1}{1-\nu^2}\left[E_5 - \frac{E_2E_4}{E_1} - c_1\left(E_7 - \frac{E_4^2}{E_1}\right)\right]\frac{\partial^3 \phi_y}{\partial y^3}$$
$$+c_1\left[\left(\frac{1}{1+\nu} + \frac{\nu}{1-\nu^2}\right)\left(E_5 - \frac{E_2E_4}{E_1}\right) - c_1\left(\frac{\nu}{1-\nu^2} + \frac{1}{1+\nu}\right)\left(E_7 - \frac{E_4^2}{E_1}\right)\right]\frac{\partial^3 \phi_y}{\partial x^2\partial y},$$
$$P(x, f) = \frac{\partial^2 f}{\partial y^2}\frac{\partial^2 \mathrm{w}}{\partial x^2} - 2\frac{\partial^2 f}{\partial x\partial y}\frac{\partial^2 \mathrm{w}}{\partial x\partial y} + \frac{\partial^2 f}{\partial x^2}\frac{\partial^2 \mathrm{w}}{\partial y^2} + \frac{1}{R}\frac{\partial^2 f}{\partial x^2},$$

$$L_{21}(\mathrm{w}) = \frac{c_1}{1-\nu^2}\left(c_1E_7 - \frac{c_1E_4^2}{E_1} - E_5 + \frac{E_2E_4}{E_1}\right)\left(\frac{\partial^3 \mathrm{w}}{\partial x\partial y^2} + \frac{\partial^3 \mathrm{w}}{\partial x^3}\right) - \frac{1}{2(1+\nu)}\left[\left(E_1 - 3c_1E_3\right) + c_2\left(E_3 - 3c_1E_5\right)\right]\frac{\partial \mathrm{w}}{\partial x},$$
$$L_{22}(\phi_x) = \left(\frac{1}{1-\nu^2}\frac{\partial^2 \phi_x}{\partial x^2} + \frac{1}{2(1+\nu)}\frac{\partial^2 \phi_x}{\partial y^2}\right)\left[E_3 - \frac{E_2^2}{E_1} - 2c_1\left(E_5 - \frac{E_2E_4}{E_1}\right) + c_1^2\left(E_7 - \frac{E_4^2}{E_1}\right)\right]$$
$$-\frac{1}{2(1+\nu)}\left[\left(E_1 - 3c_1E_3\right) + c_2\left(E_3 - 3c_1E_5\right)\right]\phi_x,$$
$$L_{23}(\phi_y) = \frac{1}{2(1-\nu)}\left[E_3 - \frac{E_2^2}{E_1} - 2c_1\left(E_5 - \frac{E_2E_4}{E_1}\right) + c_1^2\left(E_7 - \frac{E_4^2}{E_1}\right)\right]\frac{\partial^2 \phi_y}{\partial x\partial y},$$

$$L_{31}(\mathrm{w}) = \frac{c_1}{1-\nu^2}\left[c_1E_7 - c_1\frac{E_4^2}{E_1} - E_5 + \frac{E_2E_4}{E_1}\right]\left(\frac{\partial^3 \mathrm{w}}{\partial y^3} + \frac{\partial^3 \mathrm{w}}{\partial x^2\partial y}\right) - \frac{1}{2(1+\nu)}\left[E_1 - 3c_1E_3 + c_2\left(E_3 - 3c_1E_5\right)\right]\frac{\partial \mathrm{w}}{\partial y},$$
$$L_{32}(\phi_x) = \frac{1}{2(1-\nu)}\left[E_3 - \frac{E_2^2}{E_1} - 2c_1\left(E_5 - \frac{E_2E_4}{E_1}\right) + c_1^2\left(E_7 - \frac{E_4^2}{E_1}\right)\right]\frac{\partial^2 \phi_x}{\partial x\partial y},$$
$$L_{33}(\phi_y) = \left(\frac{1}{1-\nu^2}\frac{\partial^2 \phi_y}{\partial y^2} + \frac{1}{2(1+\nu)}\frac{\partial^2 \phi_y}{\partial x^2}\right)\left[E_3 - \frac{E_2^2}{E_1} - 2c_1\left(E_5 - \frac{E_2E_4}{E_1}\right) + c_1^2\left(E_7 - \frac{E_4^2}{E_1}\right)\right]$$
$$-\frac{1}{2(1+\nu)}\left[E_1 - 3c_1E_3 + c_2\left(E_3 - 3c_1E_5\right)\right]\phi_y,$$